

# Poly(2-thienyl)borates: An Investigation into the Coordination of Thiophene and Its Derivatives

Andrew L. Sargent,<sup>\*,†</sup> Emily P. Titus,<sup>†,‡</sup> Charles G. Riordan,<sup>\*,§</sup> Arnold L. Rheingold,<sup>||</sup> and Pinghua Ge<sup>§</sup>

Departments of Chemistry, East Carolina University, Greenville, North Carolina 27858, Kansas State University, Manhattan, Kansas 66506, and University of Delaware, Newark, Delaware 19716

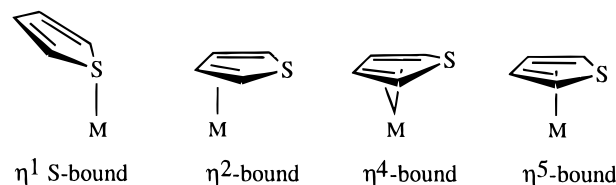
Received June 14, 1996<sup>⊗</sup>

The synthesis, characterization, and reactivity of a new sulfur-rich tridentate ligand, tetrakis(2-thienyl)borate (**1**<sup>−</sup>), are reported along with a molecular orbital analysis of its coordination to a metal center. Unlike the analogous tetrakis(methylthio)methylborate (**2**<sup>−</sup>), **1**<sup>−</sup> does not coordinate Mo(CO)<sub>3</sub> when reacted with (C<sub>7</sub>H<sub>8</sub>)Mo(CO)<sub>3</sub>. The sulfur atoms in both ligands are oriented to coordinate the metal in a pyramidal η<sup>1</sup> sulfur-bound mode. Approximate molecular orbital calculations are used to compare the metal–ligand interactions in these related species, and the results indicate that the magnitude and polarizability of the electronic charge density of the lone pairs on the sulfur atoms dictate the coordination strength of the ligands. Simple Mulliken atomic charges and orbital occupation numbers are used to determine the extent of charge delocalization. While the conjugation of the sulfur lone pair electrons with adjacent π bonds in the ligands decreases the corresponding Lewis basicity, the contribution from the aromaticity in the thienyl groups is negligible. During the course of these studies, the structure of K[**1**] was determined by X-ray diffraction. K[**1**]: monoclinic space group C2/c, with *a* = 16.00(2) Å, *b* = 7.680(7) Å, *c* = 16.22(2) Å, β = 118.520(7)°, *V* = 1750(3) Å<sup>3</sup>, *Z* = 4, *R*(*F*) = 0.0494, and *R*<sub>w</sub>(*F*<sup>2</sup>) = 0.122. The crystal lattice contains one-dimensional chains of **1**<sup>−</sup> bridged by K ions.

## Introduction

Recent studies of the interactions between transition metal ions and thiophene have revealed a subtle and diverse coordination chemistry.<sup>1</sup> The motivation for these studies has been, to a large extent, an understanding of the mechanism of catalytic hydrosulfurization (HDS), an industrial process by which sulfur is removed from petroleum feedstock.<sup>2</sup> Of the sulfur-

Chart 1



containing compounds targeted in the HDS process, thiophenes are among the most difficult to desulfurize and are therefore of particular interest. The study of the diverse coordination chemistry of thiophene and its derivatives is a popular approach to the investigation of the initial steps of the HDS mechanism. Several types of thiophene coordination to single transition metal centers are known and the structural types are summarized in Chart 1. Prior to 1985, only complexes of the η<sup>5</sup> coordination mode were known. Since then, however, complexes exhibiting η<sup>4</sup>, η<sup>2</sup>, and η<sup>1</sup> coordination modes have been discovered and all of these, including the η<sup>5</sup> mode, have been implicated as important intermediates in the HDS process.

Two general varieties of mechanisms for the C–S cleavage reaction have been proposed, one of which involves an initial π coordination of thiophene through an η<sup>5</sup>, η<sup>4</sup>, or η<sup>2</sup> binding mode and the other of which involves the initial σ coordination of thiophene through the η<sup>1</sup> S-bound mode. While both general mechanisms proceed to insert the metal into the carbon–sulfur bond, recent studies have provided evidence that the η<sup>2</sup> binding mode does not lead directly to the C–S bond activation product but arrives at this end, instead, by first rearranging to form the η<sup>1</sup> coordinated complex.<sup>3</sup> These results, along with the numerous recent reports of η<sup>1</sup> coordinated thiophene complexes, clearly underscore the importance of the η<sup>1</sup> binding mode, yet

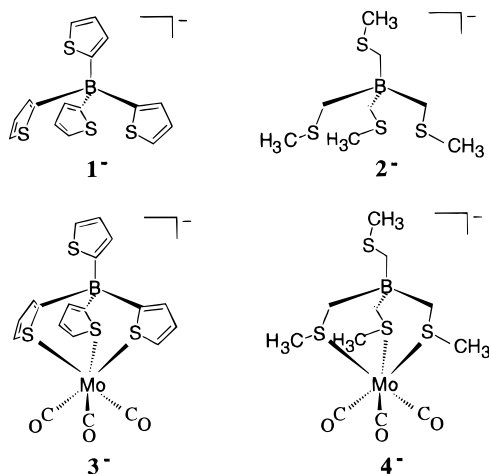
- <sup>†</sup> East Carolina University.  
<sup>‡</sup> American Chemical Society–Petroleum Research Fund Scholar.  
<sup>§</sup> Kansas State University.  
<sup>||</sup> University of Delaware.  
<sup>⊗</sup> Abstract published in *Advance ACS Abstracts*, November 1, 1996.  
 (1) See, for example: (a) Angelici, R. J. *Acc. Chem. Res.* **1988**, *21*, 387–394. Choi, M-G.; Angelici, R. J. *J. Am. Chem. Soc.* **1989**, *111*, 8753–8754. (b) Angelici, R. J. *Coord. Chem. Rev.* **1990**, *105*, 61–76. (c) Chen, J.; Daniels, L. M.; Angelici, R. J. *J. Am. Chem. Soc.* **1990**, *112*, 199–204. (d) Rauchfuss, T. B. *Prog. Inorg. Chem.* **1991**, *39*, 259–329. (e) Jones, W. D.; Dong, L. *J. Am. Chem. Soc.* **1991**, *113*, 559–564. (f) Chen, J.; Daniels, L. M.; Angelici, R. J. *J. Am. Chem. Soc.* **1991**, *113*, 2544–2552. (g) Choi, M-G.; Robertson, M. J.; Angelici, R. J. *J. Am. Chem. Soc.* **1991**, *113*, 4005–4006. (h) Barbaro, P.; Bianchini, C.; Meli, A.; Peruzzini, M.; Vacca, A.; Vizza, F. *Organometallics* **1991**, *10*, 2227–2238. (i) Choi, M-G.; Angelici, R. J. *Organometallics* **1991**, *10*, 2436–2442. (j) Bleeke, J. R.; Ortwerth, M. F.; Chiang, M. Y. *Organometallics* **1992**, *11*, 2740–2743. (k) Choi, M-G.; Angelici, R. J. *Organometallics* **1992**, *11*, 3328–3334. (l) Benson, J. W.; Angelici, R. J. *Organometallics* **1993**, *12*, 680–687. (m) Bianchini, C.; Meli, A.; Peruzzini, M.; Vizza, F.; Frediani, P.; Herrera, V.; Sanchez-Delgado, R. A. *J. Am. Chem. Soc.* **1993**, *115*, 2731–2742. (n) Bianchini, C.; Meli, A.; Peruzzini, M.; Vizza, F.; Frediani, P.; Herrera, V.; Sanchez-Delgado, R. A. *J. Am. Chem. Soc.* **1993**, *115*, 7505–7506. (o) Bianchini, C.; Barbaro, P.; Meli, M.; Peruzzini, M.; Vacca, A.; Vizza, F. *Organometallics* **1993**, *12*, 2505–2514. (p) Jones, W. D.; Chin, R. M. *J. Am. Chem. Soc.* **1994**, *116*, 198–203. (q) Bianchini, C.; Meli, A.; Peruzzini, M.; Vizza, F.; Moneti, S.; Herrera, V.; Sanchez-Delgado, R. A. *J. Am. Chem. Soc.* **1994**, *116*, 4370–4381. (r) Bianchini, C.; Frediani, P.; Herrera, V.; Jimenez, M. V.; Meli, A.; Rincon, L.; Sanchez-Delgado, R. A.; Vizza, F. *J. Am. Chem. Soc.* **1995**, *117*, 4333–4346. (s) Koczaja Dailey, K. M.; Rauchfuss, T. B.; Rheingold, A. L.; Yap, G. P. A. *J. Am. Chem. Soc.* **1995**, *117*, 6396–6397. (t) Selmezy, A. D.; Jones, W. D.; Osman, R.; Perutz, R. N. *Organometallics* **1995**, *14*, 5677–5685. (u) Chen, J.; Daniels, L. M.; Angelici, R. J. *Organometallics* **1996**, *15*, 1223–1229.

(2) Gates, B. C.; Katzer, J. R.; Schuit, G. C. A. *Chemistry of Catalytic Processes*; McGraw-Hill: New York, 1979.

(3) Dong, L.; Duckett, S. B.; Ohman, K. F.; Jones, W. D. *J. Am. Chem. Soc.* **1992**, *114*, 151–160.

relatively little is known about its coordination strength or the contributing electronic factors.

To gain a deeper understanding of  $\eta^1$  coordination to metal ions, we have prepared a new sulfur-rich anion, tetrakis(2-thienyl)borate,  $\text{B}(\text{C}_4\text{H}_3\text{S})_4^-$  ( $\mathbf{1}^-$ ), which is the thiophene analogue of the polythioether ligand tetrakis((methylthio)methyl)borate,  $\text{B}(\text{CH}_2\text{SCH}_3)_4^-$  ( $\mathbf{2}^-$ ) recently reported by one of us.<sup>4</sup>



Like the latter ligand, the former was designed to provide a relatively soft, face-capping coordination sphere. In contrast to  $\mathbf{2}^-$ , which binds avidly to a variety of metal ions in the intended manner,  $\mathbf{1}^-$  shows no affinity for the same metal fragments.

Herein we report the preparation and molecular structure of  $\text{K}[\mathbf{1}]$ . In addition, we report a theoretical comparison of the bonding in transition metal derivatives of the parent tetrakis(thienyl) and tetrakis((methylthio)methyl) ligands,  $[\mathbf{1}]\text{Mo}(\text{CO})_3^-$  ( $\mathbf{3}^-$ ) and  $[\mathbf{2}]\text{Mo}(\text{CO})_3^-$  ( $\mathbf{4}^-$ ). That the thioether moieties coordinate more strongly to metal species than thiophene moieties is an expected conclusion. What remains to be answered is why  $\eta^1$  S-bound thiophene is such a poorly coordinating ligand. While a number of important theoretical studies of the thiophene HDS reaction have been reported,<sup>5–8</sup> most have examined models of reactor,<sup>5</sup> surface,<sup>6</sup> or cluster species<sup>7</sup> where, due to the complexity of the size of these systems, the approximations have been necessarily severe. Other theoretical studies have exploited the simplicity of homogeneous organometallic model complexes and have focused on the energetics<sup>8a</sup> and nature<sup>8b,c</sup> of the orbital interactions between thiophene and a number of metal species. In the present study, the factors which govern the strength of the thiophene  $\eta^1$  bonding mode are directly examined through the comparison of the coordination chemistry of a series of related ligands.

**Table 1.** Crystallographic Data for  $\text{K}[\mathbf{1}]$

formula	$\text{C}_{16}\text{H}_{12}\text{BKS}_4$	$\beta$ , deg	118.520(7)
fw	382.4	$V$ , $\text{\AA}^3$	1750(3)
color, habit	champagne, block	$Z$	4
crystal system	monoclinic	$T$ , K	296
space group	$C2/c$	$\lambda$ , $\text{\AA}$ (Mo K $\alpha$ )	0.710 73
$a$ , $\text{\AA}$	16.00(2)	$\rho$ (calcd), $\text{g cm}^{-3}$	1.451
$b$ , $\text{\AA}$	7.680(7)	$\mu$ , $\text{cm}^{-1}$	7.71
$c$ , $\text{\AA}$	16.22(2)	$R(F)$ , $R_w(F)^a$	0.0494, 0.122

$$^a R(F) = \frac{\sum \Delta}{\sum (F_o)}; R_w(F) = \frac{\sum [\Delta w^{1/2}]}{\sum [F_o w^{1/2}]}; \Delta = |F_o - F_c|; w^{-1} = \sigma^2(F_o) + gF_o^2.$$

## Experimental Section

**Materials.** All reagents were distilled under  $\text{N}_2$  and dried as indicated. THF,  $\text{Et}_2\text{O}$ , and benzene were freshly distilled over  $\text{Na}/\text{benzophenone}$ .  $\text{BF}_3 \cdot \text{Et}_2\text{O}$  and  $\text{LiC}_4\text{H}_3\text{S}$  (2-thienyllithium) were used as received from Aldrich Chemical Co. Elemental analyses were performed by Desert Analytics. NMR spectra were recorded on a 400 MHz Bruker spectrometer equipped with a Sun workstation.

**$\text{K}[\mathbf{2}(\text{C}_4\text{H}_3\text{S})_4]$  ( $\text{K}[\mathbf{1}]$ ).** The  $\text{K}^+$  salt was prepared according to the literature procedure.<sup>9</sup> The product was precipitated by addition of aqueous  $\text{KCl}$ . The flocculent white solid was isolated by filtration, washed with  $\text{Et}_2\text{O}$  ( $2 \times 30$  mL), and dried under vacuum. Yields: 60–80%.  $^1\text{H NMR}$  ( $\text{CD}_3\text{NO}_2$ ):  $\delta$  7.16 (m, 4 H), 6.93 (m, 4 H), 6.91 (m, 4 H). The  $\text{Bu}_4\text{N}^+$  salt was prepared by addition of  $[\text{Bu}_4\text{N}]\text{Cl}$ . Anal. Calcd (found) for  $[\text{Bu}_4\text{N}][\mathbf{1}]$ ,  $\text{C}_{32}\text{H}_{48}\text{BNS}_4$ : C, 65.67 (65.73); H, 8.26 (8.49); N, 2.39 (2.37).

**Attempted Preparation of Metal Complexes.** Using synthetic protocols outlined previously,<sup>4</sup> we tried to prepare the following complexes:  $[\mathbf{1}]_2\text{M}$  ( $\text{M} = \text{Fe}, \text{Co}, \text{Ni}$ ),  $\text{K}[\mathbf{1}]\text{Mo}(\text{CO})_3$ , and  $[\mathbf{1}]\text{Cu}_4$ . While these routes proved successful for the poly((methylthio)methyl)borates, only starting materials were recovered when  $\text{K}[\mathbf{1}]$  was employed as ligand. Efforts to prepare the metal derivatives under more forcing conditions, i.e. refluxing  $\text{EtOH}$ ,  $\text{DMF}$ , or  $\text{THF}$ , resulted in intractable black oils.

**Crystallographic Structural Determinations.** Crystals of suitable quality for X-ray diffraction analysis were grown by diffusing  $\text{Et}_2\text{O}$  into an acetone solution containing  $\text{K}[\mathbf{1}]$ . Crystallographic data for the structures are presented in Table 1 and in the Supporting Information. Systematic absences in the diffraction data were consistent for the space groups  $Cc$  and  $C2/c$ . The possibility of a molecular 2-fold axis and  $Z = 4$  suggested the centric space group, which yielded chemically reasonable and computationally stable results. Both ions are located on a 2-fold axis. The structure was solved using direct methods, completed by subsequent difference Fourier syntheses and refined by full-matrix least-squares procedures. Semiempirical absorption corrections were applied. The atoms  $\text{S}(2)$  and  $\text{C}(7)$  were found to be statistically disordered with respect to each other in a 70/30 distribution. Each disordered atom site was assigned the identity of the major atom contributor and refined with partial carbon/sulfur occupancies. All non-hydrogen atoms were refined with anisotropic displacement coefficients. Hydrogen atoms were treated as idealized contributions. All software and sources of the scattering factors are contained in the SHELXTL (5.3) program library.<sup>10</sup>

**Theoretical Approach.** Unparametrized Fenske–Hall molecular orbital (MO) calculations<sup>11</sup> were employed to elucidate the electronic structure and bonding of the various thiophene and thioether complexes reported herein. Geometric parameters for  $\mathbf{1}^-$ ,  $\mathbf{2}^-$ , and  $\mathbf{4}^-$  were taken directly from the crystal data.<sup>4</sup> Since the transition metal complex of  $\mathbf{1}^-$  is not known, the geometric parameters for the hypothetical complex,  $\mathbf{3}^-$ , were derived from the crystal data of the free ligand ( $\mathbf{1}^-$ ) along with those from the metal tricarbonyl fragment in  $\mathbf{4}^-$ . The  $\text{Mo}–\text{S}$  bond distances in  $\mathbf{3}^-$  were set equal to those in  $\mathbf{4}^-$  (2.57  $\text{\AA}$ ).

To reduce the size of the calculations and increase the molecular point group symmetry (from  $C_1$  to  $C_3$ ), the apical thienyl or thioether group of the chelating ligand was replaced by a hydrogen atom bonded directly to boron. As a check, calculations were also performed on

- (4) (a) Riordan, C. G.; Ge, P.; Haggerty, B.; Rheingold, A. L. *J. Am. Chem. Soc.* **1994**, *116*, 8406–8407. (b) Ohrenberg, C.; Ge, P.; Schebler, P.; Riordan, C. G.; Yap, G. P. A.; Rheingold, A. L. *Inorg. Chem.* **1996**, *35*, 749–754. (c) Ohrenberg, C.; Saleem, M. M.; Riordan, C. G.; Yap, G. P. A.; Verma, A. K.; Rheingold, A. L. *J. Chem. Soc., Chem. Commun.* **1996**, 1081–1082.  
 (5) Harris, S.; Chianelli, R. R. *J. Catal.* **1984**, *86*, 400–412.  
 (6) Zonnevylle, M. C.; Hoffman, R.; Harris, S. *Surf. Sci.* **1988**, *199*, 320–360.  
 (7) Diemann, E.; Weber, Th.; Müller, A. *J. Catal.* **1994**, *148*, 288–303.  
 (8) (a) Rincón, L.; Terra, J.; Guenzburger, D.; Sánchez-Delgado, R. A. *Organometallics* **1995**, *14*, 1292–1296. (b) Sánchez-Delgado, R. A.; Herrera, V.; Rincón, L.; Andriollo, A.; Martín, G. *Organometallics* **1994**, *13*, 553–561. (c) Harris, S. *Organometallics* **1994**, *13*, 2628–2640.

(9) Pacey, G. E.; Moore, C. E. *Anal. Chim. Acta* **1979**, *105*, 353–359.

(10) G. Sheldrick. Siemens XRD, Madison, WI.

(11) Hall, M. B.; Fenske, R. F. *Inorg. Chem.* **1972**, *11*, 768–775.

the full complexes in the lower point group symmetry; no significant differences were observed.

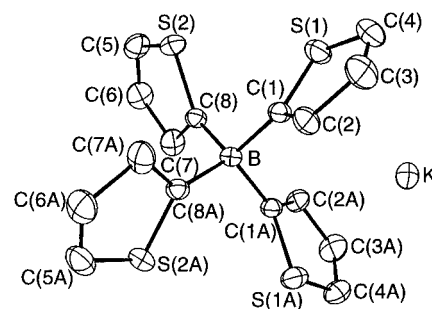
Geometries for the 2,3-dihydrothiophenic derivatives of  $3^-$ , as well as those derivatives in which the thiophene heterocycle was broken, were defined as follows. Full-gradient ab initio geometry optimizations<sup>12</sup> were performed at the RHF/6-31G level of theory on the isolated thiophenic moieties (**9**–**12**) in which a terminal C–H bond replaced the C–B bond. The geometries of these fragments were then incorporated into the parent borate ligand species for subsequent calculations of the coordination complex. The Mo–S and C–B bond distances in these hypothetical complexes were again set to those found in  $3^-$  and  $4^-$  (2.57 and 1.62 Å, respectively). For the comparisons of coordination strengths between these hypothetical derivatives of the coordination complexes and the coordination complexes involving  $1^-$  and  $2^-$ , the geometries of  $1^-$  and  $2^-$  also utilized RHF optimized parameters for the thiophene components (**9**) and methyl sulfide components, respectively, rather than the parameters taken from the X-ray data. These changes, manifest primarily in longer S–C bond distances, resulted in only minor quantitative differences in the amount of electron density transferred between the metal and borate fragments but were necessary for the consistency of the comparison.

The basis functions for all non-hydrogen atoms were generated by the numerical X $\alpha$  atomic orbital program of Herman and Skillman<sup>13</sup> used in conjunction with the X $\alpha$ -to-Slater basis program of Bursten and Fenske.<sup>14</sup> Non-transition metal atoms assumed ground-state atomic configurations, while a  $d^5s^0$  cationic configuration was used for Mo. The exponents for the valence s and p orbitals of Mo were determined by minimizing the energy difference between the valence eigenvalues obtained from molecular calculations and experimental ionization potentials.<sup>15</sup> The numerical X $\alpha$  atomic orbitals were fit to double- $\zeta$  analytical Slater type functions for the valence d orbitals of Mo and for the valence p orbitals of the other atoms except hydrogen, the exponent of which was 1.20. All other orbitals were represented as single- $\zeta$  functions. A Mulliken population analysis<sup>16</sup> was used in the calculations to determine gross and overlap populations, as well as individual atomic charges.

## Results and Discussion

**Molecular Structure of K[1].** K[1] was prepared in good yield according to the procedure of Pacey and Moore.<sup>9</sup> KCl was used in place of CsCl to precipitate  $1^-$  from aqueous solutions. Recrystallization from acetone–Et<sub>2</sub>O yielded colorless blocks suitable for X-ray diffraction analysis. K[1] crystallized in the monoclinic space group *C2/c*. The molecular structure is contained in Figure 1 with selected metric parameters in Table 2. The molecular structure consists of intimate, ionic pairs of K cations and **1** anions. The geometry about B is tetrahedral with C–B–C angles ranging from 106.8 to 111.9°. The B–C bond distances (1.63(1) Å) are ca. 0.025 Å shorter than in  $[2]_2M$  ( $M = Fe, Co, Ni$ ).<sup>4b</sup> These differences may be attributed to the different hybridizations at the C atoms. The C–C distances in the thienyl backbones deviate significantly from those in the parent thiophene (C(1)–C(2), 1.370 Å; C(2)–C(3), 1.424 Å).<sup>17</sup> Coordination to B increases the C(1)–C(2) distance to 1.416(10) Å while the C(3)–C(4) distance decreases to 1.331(13) Å. The C(2)–C(3) bond distance also increases slightly (1.436(10) Å). Each K ion is surrounded by four thienyl rings, two from one borate and two from an adjacent borate, in a pseudotetrahedral geometry. The thienyl rings are  $\eta^5$  with respect to the K ion with K–ring atom distances ranging from

A



B

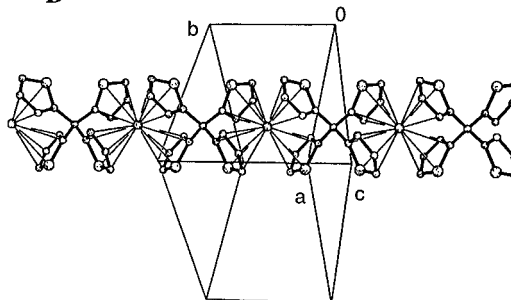
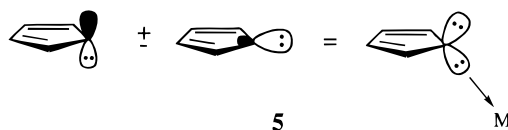


**Figure 1.** (A) Thermal ellipsoid plot of K[1]. Thermal ellipsoids are drawn at the 40% probability level. Hydrogen atoms are omitted for clarity. (B) Depiction of infinite chains of K[1] in the crystal lattice.

3.161 to 3.289 Å. This arrangement results in infinite chains of  $1^-$  bridged by K ions in the crystal lattice, Figure 1B.

**Reaction of K[1] with Metal Complexes.** K[1] does not react with  $(C_7H_8)Mo(CO)_3$ ,  $Fe(BF_4)_2 \cdot 6H_2O$ ,  $Ni(BF_4)_2 \cdot 6H_2O$ , or  $Cu(CH_3CN)_4(PF_6)$ . This is in contrast to the behavior of  $[Bu_4N][2]$ , which reacts rapidly with each of these metal complexes to yield isolable derivatives in which three S donors per borate are bound to the metal ion.<sup>4</sup>

**Molecular Orbital Calculations.** Before the interactions between the molecular fragments of the coordination complexes are discussed, it is useful to describe the molecular orbitals (MOs) of the chelating ligands with respect to the orbitals of their thiophene and thioether building blocks. Much of the bonding between the larger chelates and the metal species can be described in terms of simple linear combinations of these smaller moieties. Of the valence orbitals for thiophene and methyl sulfide illustrated in Figure 2, those which play a significant role in binding to transition metal centers through the sulfur atom are the  $2a_1$  and  $2b_1$  orbitals of the former and the  $1a_1$  and  $1b_1$  orbitals of the latter. These orbitals combine to form what can be regarded as two hybridized lone pair orbitals, one of which is used to coordinate to a metal species resulting in the known trigonal pyramidal geometry around the sulfur atom, **5**.



Three pairs of these  $a_1$  and  $b_1$  symmetry orbitals combine to form the six molecular orbitals of the tridentate borate fragments  $1^-$  and  $2^-$ , illustrated on the sides of the molecular orbital diagram shown in Figure 3. For the thioether fragment,  $2^-$ , the totally symmetric combinations of the  $1a_1$  and  $1b_1$  orbitals of methyl sulfide give rise to the  $1a$  and  $2a$  fragment molecular

(12) Pulay, P. *Mol. Phys.* **1969**, *17*, 197–204.

(13) Herman, F.; Skillman, S. *Atomic Structure Calculations*; Prentice-Hall: Englewood Cliffs, NJ, 1963.

(14) Bursten, B. E.; Fenske, R. F. *J. Chem. Phys.* **1977**, *67*, 3138–3145. Bursten, B. E.; Jensen, R. J.; Fenske, R. F. *J. Chem. Phys.* **1978**, *68*, 3320–3321.

(15) Grant, S.; Sargent, A. L.; Hall, M. B. Unpublished results.

(16) Mulliken, R. S. *J. Chem. Phys.* **1955**, *23*, 1833–1840, 1841–1846.

(17) Bak, B.; Christensen, D.; Hansen-Nygaard, L.; Rastrup-Andersen, J. R. *J. Mol. Spectrosc.* **1961**, *7*, 58–67.

**Table 2.** Selected Bond Lengths (Å) and Angles (deg) for K[1]<sup>a</sup>

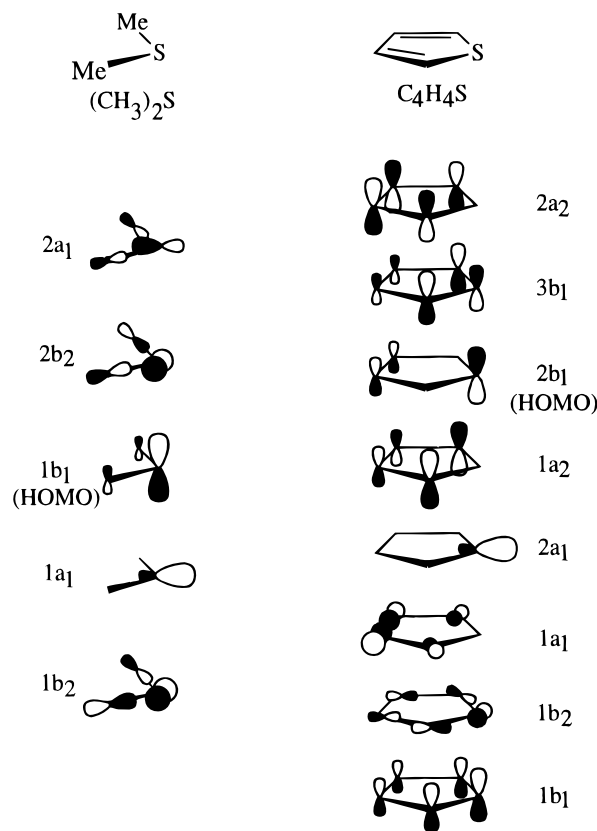
K–C(1)	3.153(4)	S(2)–K#4	3.291(2)
K–C(1)#1	3.153(4)	B–C(8)#1	1.621(5)
K–C(8)#2	3.154(4)	B–C(8)	1.621(5)
K–C(8)#3	3.154(4)	B–C(1)	1.633(5)
K–C(2)	3.220(5)	B–C(1)#1	1.633(5)
K–C(2)#1	3.220(5)	C(1)–C(2)	1.407(5)
K–C(7)#2	3.227(4)	C(2)–C(3)	1.438(6)
K–C(7)#3	3.227(4)	C(3)–C(4)	1.342(7)
K–C(6)#2	3.271(5)	C(5)–C(6)	1.336(7)
K–C(6)#3	3.271(5)	C(5)–K#4	3.297(5)
K–S(1)#1	3.274(2)	C(6)–C(7)	1.498(5)
K–S(1)	3.274(2)	C(6)–K#4	3.271(5)
S(1)–C(4)	1.689(5)	C(7)–C(8)	1.528(4)
S(1)–C(1)	1.725(4)	C(7)–K#4	3.227(4)
S(2)–C(5)	1.655(5)	C(8)–K#4	3.154(4)
S(2)–C(8)	1.712(4)		
C(1)–K–C(2)#1	66.64(11)	C(6)#2–K–S(1)	121.62(10)
C(2)–K–C(2)#1	88.9(2)	S(1)#1–K–S(1)	95.71(8)
C(1)–K–C(7)#2	117.88(9)	C(4)–S(1)–C(1)	94.0(2)
C(2)–K–C(7)#2	92.75(10)	C(4)–S(1)–K	76.1(2)
C(2)#1–K–C(7)#2	160.81(9)	C(1)–S(1)–K	70.58(13)
C(2)–K–C(7)#3	160.81(9)	C(5)–S(2)–C(8)	94.7(2)
C(2)#1–K–C(7)#3	92.74(10)	C(8)–B–C(1)	112.0(2)
C(7)#2–K–C(7)#3	91.93(12)	C(2)–C(1)–B	128.2(3)
C(1)–K–C(6)#2	105.03(11)	C(2)–C(1)–S(1)	109.3(3)
C(1)–K–C(6)#3	116.46(11)	B–C(1)–S(1)	121.9(2)
C(1)#1–K–C(6)#3	105.02(11)	C(2)–C(1)–K	79.9(2)
C(8)#2–K–C(6)#3	91.18(12)	B–C(1)–K	102.4(2)
C(2)–K–C(6)#3	136.05(11)	S(1)–C(1)–K	78.35(13)
C(7)#2–K–C(6)#3	110.83(12)	C(1)–C(2)–C(3)	111.1(4)
C(6)#2–K–C(6)#3	134.4(2)	C(1)–C(2)–K	74.6(2)
C(8)#2–K–S(1)#1	115.74(8)	C(3)–C(2)–K	80.2(3)
C(8)#3–K–S(1)#1	141.93(7)	C(4)–C(3)–C(2)	114.2(4)
C(2)–K–S(1)#1	74.39(10)	C(4)–C(3)–K	78.6(3)
C(7)#2–K–S(1)#1	115.87(8)	C(2)–C(3)–K	74.3(2)
C(7)#3–K–S(1)#1	119.77(8)	C(3)–C(4)–S(1)	111.4(3)
C(6)#2–K–S(1)#1	89.73(10)	C(3)–C(4)–K	77.9(3)
C(6)#3–K–S(1)#1	121.62(10)	S(1)–C(4)–K	74.1(2)
C(8)#2–K–S(1)	141.93(7)	C(6)–C(5)–S(2)	113.8(3)
C(8)#3–K–S(1)	115.74(8)	C(5)–C(6)–C(7)	116.4(4)
C(2)–K–S(1)	46.45(9)	C(6)–C(7)–C(8)	103.9(3)
C(2)#1–K–S(1)	74.39(10)	C(7)–C(8)–B	126.4(2)
C(7)#2–K–S(1)	119.77(8)		

<sup>a</sup> Symmetry transformations used to generate equivalent atoms: (#1)  $-x + 2, y, -z + 3/2$ ; (#2)  $-x + 2, y - 1, -z + 3/2$ ; (#3)  $x, y - 1, z$ ; (#4)  $x, y + 1, z$ .

orbitals (FMOs), while the remaining symmetry-adapted combinations give rise to the 1e and 2e sets of doubly degenerate FMOs. Notice that the 2e FMO of **2**<sup>-</sup> is the HOMO for the isolated fragment.

The FMOs of **1**<sup>-</sup> are constructed similarly. The principal difference is that the six FMOs which are formed from the symmetry-adapted linear combinations of the 2a<sub>1</sub> and 2b<sub>1</sub> orbitals of the three thiophene moieties do not correspond to the six highest occupied FMOs of **1**<sup>-</sup>, as was the case in **2**<sup>-</sup>. More importantly, the 2e FMO of **1**<sup>-</sup> is not the HOMO of the fragment but rather has three occupied FMOs above it energetically. These three FMOs correspond to the a- and e-type symmetry combinations of the thiophene 1a<sub>2</sub> orbital. The 2a FMO of **1**<sup>-</sup>, which is not shown in Figure 3, is primarily boron in character and resides directly above the 1a FMO.

One of the most important interactions between the ligands and the metal involves the 3e orbitals of the metal fragment and the 2e orbitals of the borate ligand. In the vernacular of the coordination chemist, this interaction represents the primary components of the Lewis acid/Lewis base chemistry; the borate orbitals are the electron donors and metal orbitals are the acceptors. The energy difference between the 3e orbitals of the metal fragment and the 2e orbitals of **1**<sup>-</sup> is 1.5 eV greater than that with the 2e orbitals of **2**<sup>-</sup>. One way of quantifying

**Figure 2.** Character, symmetry, and energetic ordering of the valence molecular orbitals of thiophene and methyl sulfide in C<sub>2v</sub> symmetry.

the extent of interaction between two atomic or fragment molecular orbitals is through a second-order perturbation correction to the molecular energy,<sup>18</sup> eq 1. The numerator of

$$E_i^{(2)} = \sum_{j \neq i} \frac{|H'_{ij}|^2}{E_i - E_j} \quad (1)$$

this expression, the square of the Fock matrix element, is a term which depends on orbital overlaps, while the denominator is the difference in energy between the interacting fragment molecular orbitals. The greater energy difference between the 2e orbitals of **1**<sup>-</sup> and the 3e orbitals of Mo(CO)<sub>3</sub> therefore translates into a weaker interaction between the two fragments.

The Mulliken gross populations, listed in Table 3, reflect the weaker coordination of **1**<sup>-</sup>; the metal 3e FMO, which was unoccupied prior to the interaction, gains only 0.27 electron from fragment **1**<sup>-</sup> while it gains 0.31 electron from fragment **2**<sup>-</sup>. Notice that the participation of the 3e orbitals of **1**<sup>-</sup> (not shown in Figure 3) as Lewis bases is largely a consequence of the symmetry-allowed mixing of the 2e and 3e orbitals. Linear combinations of these orbitals can separate the contributions arising from the 2b<sub>1</sub> and 1a<sub>2</sub> MOs of the thiophene moieties.

The calculations presented in Figure 3 do little more than corroborate a known experimental result. Of greater interest is an understanding of the chemical factors which influence the coordination strength of sulfur-containing ligands. We have indicated that the energy difference between the borate 2e orbitals and the metal 3e orbitals influences the extent of the interaction but have said nothing about the origin of this difference or about the possible influence of the overlap terms in the numerator of eq 1. To address these issues, we focus on

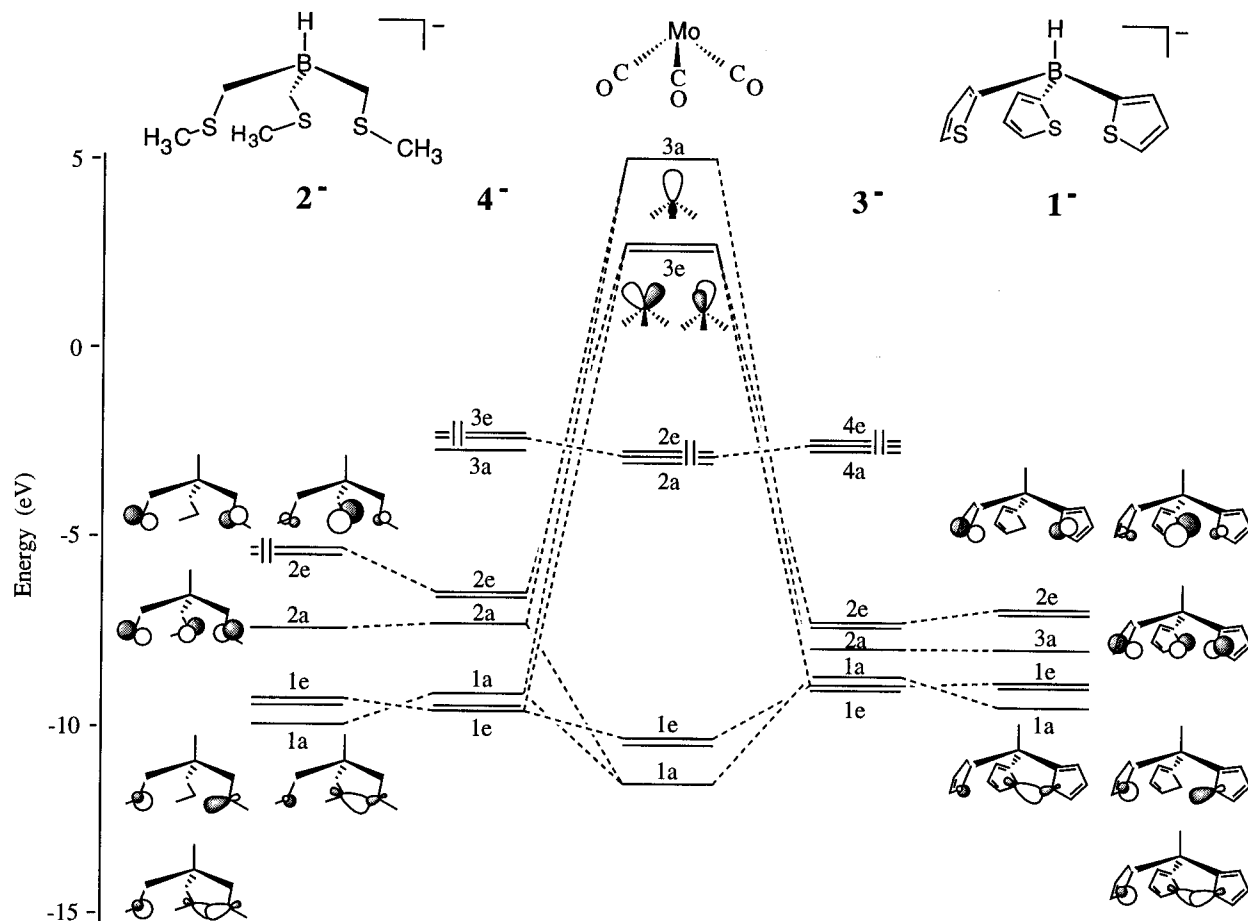
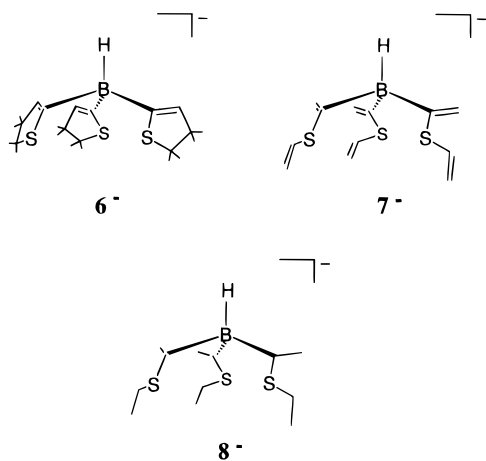


**Figure 3.** Molecular orbital diagram for the coordination complexes  $3^-$  and  $4^-$ . The orbital energies of  $1^-$  were scaled such that the energies of the  $\text{Mo}(\text{CO})_3$  fragment molecular orbitals were the same as those in the coordination complex involving  $2^-$ . Only the orbitals of the sulfur atoms are shown for clarity.

the separate contributions made by the heterocyclic nature of thiophene and its aromaticity.

Calculations involving three species closely related to  $1^-$ , the molecular structures of which are illustrated in  $6^-$ – $8^-$ , have been performed to determine the effects of both the aromaticity



and the heterocycle on the coordination strength of the chelating ligand. In each case, the coordination strength was estimated by the amount of electron density donated from the chelating ligand to the 3e and 3a orbitals of the  $\text{Mo}(\text{CO})_3$  fragment; the sum of the Mulliken gross populations of these metal orbitals are listed at the bottom of Table 4. Relative to  $1^-$ , both the ethyl sulfide derivative,  $8^-$ , and the 2,3-dihydrothiophene derivative,  $6^-$ , donate more electron density (0.05 and 0.02

**Table 3.** Mulliken Gross Populations of the FMOs of  $1^-$ ,  $2^-$ , and  $\text{Mo}(\text{CO})_3$  for the Interactions Leading to the Coordination Complexes ( $3^-$  and  $4^-$ ) Illustrated in Figure 3, Along with Orbital Symmetries in Parentheses

	$4^-$		$3^-$	
	$2^-$	$\text{Mo}(\text{CO})_3$	$\text{Mo}(\text{CO})_3$	$1^-$
(2e)	1.74	(3a) 0.14	(3a) 0.11	(4a) 2.00
(2a)	1.96	(3e) 0.31	(3e) 0.27	(3e) 1.87
(1e)	1.95			(2e) 1.93
(1a)	1.85			(3a) 2.00
				(1e) 1.91
				(2a) 1.98
				(1a) 1.85

**Table 4.** Energy Difference (eV) between the 3a and 3e FMOs of  $\text{Mo}(\text{CO})_3$  and the Six FMOs from the Ligands Involved in  $\eta^1$  S-Bound Coordination, Along with the Total Donation of Electron Density from the Tridentate Ligands Calculated from the Sum of the Mulliken Gross Populations of the 3a and 3e FMOs of  $\text{Mo}(\text{CO})_3$

FMO symm	ligand				
	$1^-$	$2^-$	$6^-$	$7^-$	$8^-$
e	9.45	8.61	8.26	8.00	8.27
a	13.13	12.59	11.55	12.08	11.86
e	12.18	12.30	12.74	12.46	11.23
a	14.93	14.96	15.33	14.78	14.97
tot. donation	0.36	0.43	0.38	0.35	0.41

electron, respectively) to the metal fragment, while the ethylene sulfide derivative,  $7^-$ , donates less ( $-0.01$  electron). The relative coordination strength of the ligands therefore follows the order  $7^- < 1^- < 6^- < 8^-$ . That the two extremes both contain acyclic organosulfur moieties implies that the hetero-

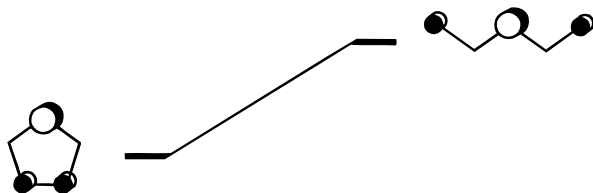


**Figure 4.** Comparison of the relative energies of the  $2b_1$  orbital of thiophene before and after the heterocycle is broken.

cyclic nature of thiophene does not play an important role in determining its effectiveness as a Lewis base. From an energetics standpoint, we expect that as the heterocycle of thiophene breaks, the  $2b_1$  MO becomes less stable due to the loss of the bonding interaction between the distal carbon atoms, as shown in Figure 4. This destabilization favors an enhanced interaction with the  $3e$  and  $3a$  FMOs of the metal fragment but alone does not provide a sufficient driving force to promote the strong interaction between the Lewis acid and Lewis base, as evident in the case of  $7^-$ . If it did, we would expect  $7^-$  to coordinate strongly to the metal fragment.

The calculated energy differences between the ligand FMOs which involve the S  $p\pi$  or S  $sp_z$  orbitals vital to the  $\eta^1$  S-bound coordination and the  $\text{Mo}(\text{CO})_3$   $3e$  and  $3a$  FMOs are listed in Table 4 for the various ligands under consideration. Notice that, despite the predominantly smaller energy differences involving the metal complex of  $7^-$  relative to  $1^-$ , the magnitude of the Lewis acid–Lewis base interaction is smaller. Indeed, the splittings associated with complex  $7^-$ , which is the complex with the weakest coordination, are significantly less than those associated with  $2^-$ , the complex with the strongest coordination. This comparison clearly indicates that the energy splitting between interacting fragments does not dictate the overall strength of the Lewis acid Lewis base interaction, as the results from Figure 3 might suggest, but, by exclusion, implies that some property based on orbital overlap dominates the interaction chemistry. Electron delocalization is a likely candidate.

While the aromaticity is lost in each of the three derivatives  $6^-$ – $8^-$ , a significant amount of stabilization, due to the delocalization of the lone pair electrons on sulfur through conjugation with the available carbon–carbon double bonds, is present in  $7^-$  and, to a lesser extent, in  $6^-$ . The conjugation is greatest in  $1^-$ , with contributions from two double bonds and the aromaticity for each thiophenic moiety. Ligands  $7^-$ ,  $6^-$ , and  $8^-$  have two, one, and no double bonds per thio group, respectively. The localization of the sulfur electronic charge density, which is a consequence of this conjugation, therefore follows the order  $1^- < 7^- < 6^- < 8^-$  and comes close to corresponding directly to the coordination strength of the ligands. Assuming that a perfect correspondence existed, these results suggest that the greater the localization of the sulfur lone pairs and, hence, the more electron density localized on the sulfur atom, the stronger the Lewis base. However, the relationship is not perfect, and we must reconcile the apparent deviation from the trend exhibited in ligands  $7^-$  and  $1^-$ .

Calculations on the isolated sulfur-containing moieties, independent of the parent borate ligands, were performed, and the results are presented in Figure 5 and Table 5. The calculated atomic charges on the sulfur atom provide an approximate measure of the delocalization of the sulfur lone pairs. Notice that the calculated charges in the isolated species  $9$ – $12$  reflect the trend of electron delocalization in the parent borate ligands: given in the order of decreasing atomic charges, the trend  $9 > 11 > 10 > 12$  matches the trend in the respective parent ligands,  $1^- > 7^- > 6^- > 8^-$ . Notice, too, that there is qualitative agreement in the calculated atomic charges regardless

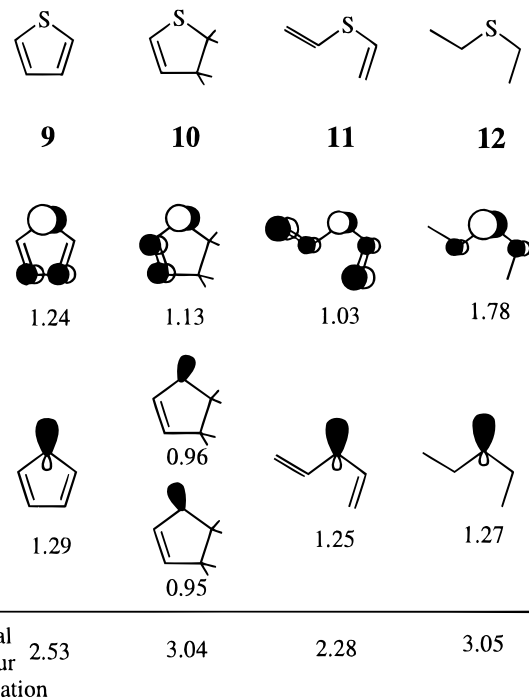


**Figure 5.** Comparison of the character and sulfur atomic populations for the occupied molecular orbitals which play a significant role in the S-bound  $\eta^1$  coordination to metal centers for species  $9$ – $12$ . The results were obtained from ab initio calculations at the RHF/6-31G level of theory.

**Table 5.** Sulfur Atomic Charges<sup>a</sup> Relative to Isolated Thiophene ( $9$ ) or Tetrakis(2-thienyl)borate ( $1^-$ )

method	molecule			
	9	10	11	12
ab initio	0	-0.158	-0.042	-0.254
Fenske–Hall	0	-0.209	-0.105	-0.272
method	ion			
	$1^-$	$6^-$	$7^-$	$8^-$
Fenske–Hall	0	-0.193	-0.067	-0.232

<sup>a</sup> Atomic charges are determined from Mulliken gross populations.

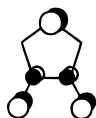
of the method used (ab initio or Fenske–Hall) or the model employed (full borate ligand,  $1^-$ ,  $6^-$ – $8^-$ , or isolated fragment,  $9$ – $12$ ).

The weaker coordination of  $7^-$  relative to  $1^-$  can be understood from the molecular orbital contributions to the atomic charges. Figure 5 illustrates the molecular orbitals most important to the  $\eta^1$  coordination mode; the S  $p\pi$  MO, which is perpendicular to plane of the thiophene unit, and the S  $sp_z$  hybrid, which lies in the plane. In spite of the more negative sulfur atomic charge in  $11$  relative to  $9$  (Table 5), the sulfur atomic population (or occupation number) in the S  $p\pi$  MO of  $11$  (the HOMO) is less than that of the corresponding S  $p\pi$  orbital of  $9$  (the SHOMO). Relative to that in  $9$ , the sulfur character in the high-lying occupied  $p\pi$  MO is smaller in  $11$  and translates into a smaller atomic population for this orbital which is important to the  $\eta^1$  coordination mode. Since the total atomic charge is calculated from the difference of the atomic number and the total gross atomic population (summed over all occupied MOs),<sup>19</sup> this means that more of the total atomic population in  $11$  resides in low-lying MOs. The principal

(19) Levine, I. N. *Quantum Chemistry*, 3rd ed.; Allyn and Bacon: Newton, MA, 1983; p 433.

characteristic of an effective Lewis base in this context is, therefore, that the sulfur lone pairs are localized in high-lying occupied orbitals. The sulfur occupation numbers, summed over the high-lying occupied orbitals of importance to  $\eta^1$  coordination, e.g. those shown in Figure 5, correlate with the coordination strength of the parent borate ligands,  $\mathbf{11} < \mathbf{9} < \mathbf{10} < \mathbf{12}$ , and support this conclusion.

Increasing the Lewis basicity of thiophene may result as a consequence of a disruption of the aromaticity through the hydrogenation of the unsaturated bonds or through enhancing the ring electron density by functionalization with strong donor groups (e.g. methyl, methoxy). The same objective might also be achieved by substitution in the 3,4-positions of thiophene with a strong  $\pi$  donor ligand such as a halide. This would result in a higher energy  $b_1$  orbital due to the antibonding interaction between the carbon atoms in the 3,4-positions and the respective halogens, **13**.

**13**

### Conclusions

The molecular structure of K[**1**] has been determined by X-ray diffraction. In the solid state the borates orient to form infinite chains of borate anions with bridging K ions which are  $\eta^5$ -bound to two thienyl substituents from neighboring anions. In contrast to the analogous aliphatic borate, **2**<sup>-</sup>, **1**<sup>-</sup> does not coordinate to a variety of metal ions.

A theoretical comparison of **1**<sup>-</sup> with the closely related and more reactive **2**<sup>-</sup>, suggested that an increased energetic separa-

tion in the former between the donor orbitals of the ligand fragment and the acceptor orbitals of the metal fragment was responsible for the decreased  $\eta^1$  coordination strength. However, an analysis of the bonding in the related conjugated aliphatic complex **7**<sup>-</sup> revealed that the energy separation between interacting fragments is not as important to the coordination strength of the ligand as the localization of the electronic charge density in the sulfur lone pair orbitals. Delocalization of the lone pair charge density through conjugation with adjacent  $\pi$  bonds decreases the Lewis basicity of the ligand. The additional delocalization associated with aromaticity, i.e. the extra conjugation provided by the heterocycle, is not observed in the results of the calculations and implies that the aromaticity in thiophene is weak and does not contribute significantly to the strength of the Lewis base. Consequences of the weak aromatic stability extend into the mechanism of the activation reactions involving the  $\eta^2$  coordination complex. Accurate ab initio studies which investigate the C-S and C-H bond activation reactions involving the  $\eta^2$  and  $\eta^1$  coordination complexes will be reported in another paper.<sup>20</sup>

**Acknowledgment.** A.L.S. thanks the donors of the Petroleum Research Fund, administered by the American Chemical Society (Grant 29526-GB6), for partial support of this research. C.G.R. acknowledges financial support from the National Science Foundation through a National Young Investigator Award (1994–9), the Exxon Educational Fund, and DuPont Central Research and Development.

**Supporting Information Available:** Tables giving a structure determination summary, atomic coordinates, bond lengths and bond angles, anisotropic thermal parameters, and hydrogen atom parameters for K[**1**] (6 pages). Ordering information is given on any current masthead page.

IC960703A

(20) Sargent, A. L.; Yandulov, D. V.; Titus, E. P. Manuscript in preparation.